

Space Weather on the Surface of Mars: Impact of the September 2017 Events

D.M. Hassler¹, C. Zeitlin², B. Ehresmann¹, R.F. Wimmer-Schweingruber³, J. Guo³, D. Matthiä⁴, S. Rafkin¹, T. Berger⁴, G. Reitz⁴

¹Southwest Research Institute, Boulder, CO, USA, ²Leidos Innovations Corporation, Houston, TX, USA, ³Christian Albrechts University (CAU), Kiel, Germany, ⁴German Aerospace Center (DLR), Institute of Aerospace Medicine, Cologne, Germany

Corresponding author: Donald M. Hassler (hassler@boulder.swri.edu)

Key Points:

- The surface of Mars is directly exposed to the effects of space radiation and space weather due to its thin atmosphere and lack of a global magnetic field.
- On Sept. 11, 2017, MSL RAD observed the strongest solar particle event seen on the surface of Mars since landing in 2012.
- Dose rates & neutral particle fluxes increased by factor of 2. Proton & ⁴He fluxes increased by factor of 30 and 10, respectively.
- Integrated dose was only slightly greater than before the event, due to reduced quality factor during the event, and Forbush decrease after the event.

Abstract

Although solar activity is declining as the Sun approaches solar minimum, a series of large solar storms occurred in September 2017 that impacted both Earth and Mars. This was the largest event seen on the surface of Mars by the Radiation Assessment Detector (RAD) on the Mars Science Laboratory (MSL) *Curiosity* rover since landing in 2012, and was also observed as GLE72 on Earth, making it the first event observed to produce a Ground Level Enhancement (GLE) on 2 planets at the same time. We present RAD observations of the surface radiation environment since 2012, and discuss the impact of the September 2017 events on this environment, and its implications for human exploration and for mitigating the risk of space radiation and space weather events for future manned missions to Mars.

This article has been accepted for publication and undergone full peer review but has not been through the copyediting, typesetting, pagination and proofreading process which may lead to differences between this version and the Version of Record. Please cite this article as doi: 10.1029/2018SW001959

1. Introduction

Although solar activity has been declining as the Sun approaches solar minimum, a series of large solar storms occurred in September 2017 that impacted both Earth and Mars. Between September 6-10, Active Region AR2673 produced four X-class flares accompanied by several Earth-directed coronal mass ejections (CME). On September 10, AR2673 produced an X8.2 flare and a solar particle event and CME which impacted both Earth and Mars, separated more than 170 degrees in longitude (Guo et al, 2018, Lee et al, 2018). These events produced aurorae at both Earth and Mars (Schneider et al., 2018), were observed in Low-Earth orbit by instruments aboard the International Space Station (ISS) (Berger et al. 2018), and produced the first GLE (GLE 72) seen on Earth since 2012 (Share and Murphy, 2018). Since this event was also observed by RAD on the surface of Mars, it is the first GLE observed on two planets at the same time, which is a relatively rare occurrence due to varying planetary alignment and the way that SEP propagate through the heliosphere.

The effects and impact of space weather at other planets is becoming more and more important as space research and human exploration expands out of Low-Earth orbit into the solar system. In particular, unlike Earth, the surface of Mars is much more exposed to space radiation and the effects of space weather. This is true for two reasons; 1) Mars lacks a global magnetic field or magnetosphere to deflect high energy charged particles, and 2) the Martian atmosphere is very thin (roughly two orders of magnitude smaller column density compared to Earth), providing significantly less effective shielding, as illustrated in Figure 1. As a result, exposure to the radiation environment on the surface of Mars remains a major concern and health risk for future human explorers.

The radiation environment on the surface of Mars is dominated by Galactic Cosmic Rays (GCR) and secondary particles created by GCR interacting with the atmosphere and soil on the surface. GCR are very high energy charged particles made up of roughly 87% protons, 12% helium, and ~1% heavier nuclei (Simpson et al., 1983), most of which propagate through the Martian atmosphere. GCR that reach the surface can also interact with the soil to produce albedo neutrons and other secondary particles.

The radiation environment can also be dominated, on short time scales (usually hours to days), by Solar Energetic Particles (SEP) generated at the Sun and accelerated by solar flares or shocks associated with CME. However, due to the martian atmosphere, with an average column depth of ~16 g/cm², only protons with energies above ~150 MeV at the top of the atmosphere will reach the surface. For the case of Gale Crater, located well below the mean martian surface altitude, this value is ~170 MeV. Particles with lower energy will be stopped in the atmosphere. Thus, only SEP with initial energies above this threshold can be detected directly on the surface. This time varying combination of GCR, SEP and albedo neutrons creates a complex radiation environment of charged and neutral particles on the surface of Mars (Ehresmann, et al., 2014, Koehler et al., 2014) that needs to be monitored and understood in order to fully manage and mitigate the risk to future robotic and human exploration missions.

2. The RAD Investigation

RAD (Hassler et al., 2012) is an instrument on MSL *Curiosity* rover (Grotzinger et al., 2012) that landed on Mars on Aug. 6, 2012 (Figure 2). RAD began operations and made the first measurements of the radiation environment on the surface of Mars on Aug. 7, 2012,

exactly 100 years after the discovery of cosmic rays on Earth by Victor Hess with his high altitude balloon (Forey, *NYT*, 2012). To date, RAD has been characterizing the changing radiation environment on the surface of Mars for almost 6 years (>2000 sols) (A sol is a martian “day” with a duration of ~ 24 hours 40 minutes.) (Hassler et al., 2014, Koehler et al., 2014, Ehresmann et al., 2014, Rafkin et al., 2014, Guo et al., 2015a, Wimmer-Schweingruber et al., 2015, and Zeitlin et al., 2016).

The MSL RAD instrument has been described in detail in the literature (Hassler et al. 2012, Zeitlin et al., 2016). RAD (*Figure 2*) is comprised of a solid state detector telescope and CsI calorimeter with active coincidence logic to measure charged particles ($Z=1-26$) over the energy range of a few MeV/nucleon to >100 MeV/nucleon, and separate scintillators with anti-coincidence logic to detect neutral particles (neutrons and γ -rays) over the energy range 10-100 MeV (*Figures 3, 4*). RAD also measures dose rates in silicon (Detector B) and in tissue-equivalent plastic (Detector E) for LET (linear energy transfer) of 0.2 to 800 keV/ μ m. The dosimetry triggers (one for B, one for E) accept any energy deposit above threshold in either detector. Because each of these triggers depends only on a single detector, there are no restrictions on the direction of incidence of incoming particles, enabling dose measurements with 4π steradian detector response. RAD also measures differential energy spectra for single ion species and their isotopes (e.g., protons, deuterons, and tritons) at energies below ~100 MeV/nucleon, as well as integral fluxes of charged particles with energies above 100 MeV/nucleon for different ion species (e.g., $Z=1$, $Z=2$, $Z=3-5$) as described in more detail in Ehresmann et al., 2014. Neutral particles are statistically separated into neutron and gamma-ray spectra via an inversion process described by Koehler et al., 2014. These flux and spectra measurements provide important input to validate and evaluate radiation transport model calculations of the expected radiation environment and exposures for exploration missions, from codes such as High Charge and Energy Transport (HZETRN) (Slaba et al., 2010) or PLANETOCOSMICS (Desorgher et al., 2006), a model based on GEANT4 (Agostinelli et al., 2003, Allison et al., 2006, Allison et al., 2016).

3. RAD Observations and Analysis of the September 10, 2017 Event

During the first five years of its mission, since landing on Mars on Aug. 6 2012, RAD detected five relatively modest solar particle events (SPE) on the surface of Mars (April and October 2013, January and September 2014, and October 2015 (*Figure 5*). Then, on September 10, 2017, RAD detected the largest SPE observed to date (*Figure 6*).

The event occurred in the declining phase of solar cycle 24, at a time when solar activity increased suddenly. In the days leading up to September 10, 2017, Active Region (AR) 2673 produced several X-class flares, including an X8.2 flare on September 10. Several hours after this flare activity, at approximately 19:50 UTC, RAD began to detect an increase in the surface radiation environment, indicating that SEP were accelerated to high enough energies to be able to propagate through the Martian atmosphere to the surface. The September 2017 event is of particular interest because it was not only detected by RAD on the surface of Mars, but also by other instruments in Mars orbit on MAVEN and other spacecraft. It was detected in Low-Earth Orbit (LEO) on the ISS (Berger et al. 2018), and with neutron monitors on the surface of Earth (Share & Murphy, 2018), making it the first GLE observed simultaneously on two planets.

As can be seen in Figure 7 and described in more detail by Ehresmann, et al. 2018, this SPE led to an increase in the surface proton flux (<100 MeV/nucleon) by a factor of 30, respectively by a factor of 3-4 for protons with even higher energies. The increase in the lower energy proton regime, thereby, started around an hour later compared to the higher-energy protons, owing to the longer travel time from the source to Mars of the slower protons. That the increase of the lower-energy proton flux was a factor of 10 stronger (compared to the higher-energy regime) can be attributed to the spectral shape of the incoming proton SEP spectrum which falls off with a power law with increasing energy above the 170 MeV needed for protons to reach the surface. Furthermore, the ^4He flux also showed a significant increase by a factor of 10 during the event, showing that during this event also higher-Z ions were accelerated to high enough energies to reach the Martian surface. The neutral radiation environment on Mars is created by charged particles (predominantly protons) interacting with the atmosphere and soil. As a result of the increase in charged particle flux (by the arriving SEP), the neutral particle environment, subsequently, increased by a factor of 2 during the event. The implications of this event for human exploration in terms of a detailed analysis of the radiation exposure are discussed in Zeitlin et al., 2018.

The relatively rapid rise in intensity of this SPE has implications for planning future human exploration, in which astronauts would perform expeditions in which they drive considerable distances from their habitat. A fast-onset event can in principle lead to large exposures if explorers are too far from shelter and have no contingency plan. As seen on Mars, the event was unambiguously underway by roughly 20:00 UTC on September 10, and dose rates doubled within about 7 hours. If one were relying only on monitors on the surface of Mars or in orbit, a fast-onset SPE could be problematic for long drives, particularly in the case of a more intense solar event, such as the January 20, 2005 SPE (Mewaldt et al. 2005). However, for the September 10, 2017 event, the exposure incurred by being unsheltered for the duration of the event would have been comparable to adding about two days of GCR exposure. In the context of a long-stay mission scenario (Table 1), where the surface mission would be planned to last for hundreds of days, the extra exposure would be negligible. Moreover, the Forbush decrease following the SPE mitigated this small increase even further, as discussed in the next section.

3. Radiation Quality Factors and Dose Equivalent

Because the biological damage caused by radiation does not depend only on absorbed dose (energy per unit mass), the quantity dose equivalent is often used to provide a rough estimate of the risk of induced cancer associated with exposure. In a “mixed field” of charged particles of various types and energies, dose equivalent is defined as the product of dose and the average radiation quality factor, $\langle Q \rangle$. We use the quality factor defined by ICRP Report 60 (ICRP, 1990), which depends on knowledge of the LET spectrum in water. RAD measures LET in silicon, making it necessary to convert to water. A simple scaling factor is applied to the LET spectra measured in silicon to obtain the (approximate) LET spectra in water. In solar quiet times, the average quality factor, $\langle Q \rangle$, measured by RAD on the martian surface is found to be in the range between 2 and 3 (Hassler et al. 2014, Zeitlin et al. 2018). This is entirely due to GCR and their associated secondary particles produced in nuclear interactions. The quality factor for the medium to low energy protons that dominate most solar particle event spectra is closer to $Q=1$. So although a portion of the LET spectrum from solar energetic particles during this event was greatly enhanced compared to the quiet-time GCR

spectrum, the enhancement was concentrated at low LET values, between 0.2 and 10 keV/ μm , where $Q = 1$ (Zeitlin et al. 2018). Hence the significant dose rate increase during the event yielded only about a 20% increase in dose equivalent rate compared to the GCR rates before and after the event (Table 1). The dose equivalent rate in the E detector, which is more shielded than the B detector, actually decreased by about 4% during the peak of the event compared to GCR-only rates before, due to the dilution of $\langle Q \rangle$ by the low-LET particles that dominated the event. Moreover, the Forbush decrease that immediately followed the event caused GCR dose rates in both B and E to drop by $\sim 12\%$ in the 5-day period after the event. GCR rates then recovered gradually over the next month, returning to pre-event levels by mid-October. A detailed analysis of the effect of the diluted quality factor during the event and the shielding from the Forbush decrease after the event on the integrated dose and dose equivalent is discussed in Zeitlin et al. 2018.

These results cannot be generalized to other possible SPE scenarios, which can conceivably have much more serious implications for humans exploring Mars. For the September 10 event, Mars was on the flank of the CME, and the magnetic connection between Mars and the source region on the Sun was poor. If the CME had been directed more towards Mars, or if the magnetic connection had been better, the dose rate increases during the event would likely have been much larger. Also, the atmospheric shielding above RAD in Gale crater is greater than that of the mean Martian surface. The mean martian surface or elevation is defined by measurements from the Mars Orbiter Laser Altimeter (MOLA) whereby the average value of the equipotential surface at the equator equals the mean radius of Mars (Smith et al. 2001). Gale Crater is >4 km below the mean elevation of the Martian surface, and RAD was shielded by about 23 g cm^{-2} of CO_2 atmosphere during this event, which is significantly greater than at other locations on Mars. At the mean Martian elevation, the column depth of the atmosphere is about 16 g cm^{-2} , and depending on the detailed energy spectrum of the accelerated particles, the dose and dose equivalent rates could be considerably larger. Based on calculations of the correlation between Martian pressure and measured RAD dose by Guo et al. 2015b (see equation (6) therein), the dose rate is approximately 15-20% larger at the mean Martian (MOLA) elevation compared to Gale crater under the same atmospheric and heliospheric conditions. This difference is probably larger during SPE, when mainly the intensity of lower-energy protons (<100 MeV on the surface) is increased (see Ehresmann et al, 2018), and a significant fraction of these protons will lose their remaining energy in the additional atmosphere above the surface of Gale crater (compared to mean elevation)..

4. Conclusions

RAD observed roughly a factor of two increase in dose rates due to the 10 Sept 2017 SPE on Mars, both in the lightly-shielded B detector and in the more-shielded E detector. The count rate of neutral particles in the E detector, which is likely dominated by low-energy neutrons, rose by a factor of ~ 2 during the event. For purposes of calculating dose equivalent, the decrease in Quality Factor $\langle Q \rangle$ offset the increase in dose rates, so that the dose equivalent rate was only slightly greater than during the preceding solar quiet time in the B detector, and was actually slightly below the quiet-time rate in the E detector. The Forbush decrease following the event also reduced GCR dose rates, so the integrated doses and dose equivalents for the 30-day period including the event are only slightly greater than for the 30-day period prior to the event. However, it is difficult to generalize from a single, relatively small event to other SPE scenarios. Only future observations, as we progress through the Solar Cycle, will allow us to understand these complex events. Comparison of the RAD

observations of this event at Mars with similar observations at Earth or in Earth orbit (e.g. Berger et al. 2018) are beyond the scope of this work but are available for future analysis to be reported in future publications.

Acknowledgments

RAD is supported by NASA Human Exploration and Operations Mission Directorate (HEOMD) under Jet Propulsion Laboratory (JPL) subcontract #1273039 to Southwest Research Institute and in Germany by the German Aerospace Center (DLR) and DLR's Space Administration grant numbers 50QM0501, 50QM1201 and 50QM1701 to the Christian-Albrechts-Universität zu Kiel. The data used in this paper are archived in the NASA Planetary Data System's Planetary Plasma Interactions Node at the University of California, Los Angeles. The archival volume includes the full binary raw data files, detailed descriptions of the structures therein, and higher-level data products in human-readable form. The PPI node is hosted at the following URL: <http://ppi.pds.nasa.gov>.

References

Agostinelli, S., Allison, J., Amako, K., Apostolakis, J., Araujo, H., Arce, P. al. (2003). GEANT4-a simulation toolkit. *Nuclear Instruments and Methods in Physics Research Section A*, 506(3), 250-303. [https://doi.org/10.1016/S0168-9002\(03\)01368-8](https://doi.org/10.1016/S0168-9002(03)01368-8)

Allison, J., et al. (2006). GEANT4 developments and applications, *IEEE Transactions on Nuclear Science*, 53, no. 1, doi:10.1109/TNS.2006.869826.

Allison, J., et al. (2016). Recent developments in GEANT4, *Nuclear Instruments and Methods in Physics Research A*, 835, 186-225, <https://doi.org/10.1016/j.nima.2016.06.125>.

Berger, T., D. Matthiä, S. Burmeister, R. Rios, K. Lee, E. Semones, D.M. Hassler, N. Stoffle, C. Zeitlin (2018). The Solar Particle Event on 10 September 2017 as observed on-board the International Space Station (ISS), *Space Weather*, this issue.

Desorgher, L., E.O. Flueckiger and M. Gurtner (2006). The PLANETOCOSMICS GEANT4 application, in 36th COSPAR Assembly, 36.

Ehresmann, B., D.M. Hassler, C. Zeitlin, J. Guo, J. Köhler, R. F. Wimmer-Schweingruber, J.K. Appel, D.E. Brinza, S. Rafkin, S. Böttcher, S. Burmeister, H. Lohf, C. Martin, E. Böhm, D. Matthiä, G. Reitz (2016). Charged Particle Spectra measured during the transit to Mars with the Mars Science Laboratory Radiation Assessment Detector (MSL/RAD), *Life Sciences in Space Research (LSSR)*, <http://dx.doi.org/10.1016/j.lssr.2016.07.001>.

Ehresman, B., Hassler D. M., Zeitlin, C., Guo, J., Wimmer-Schweingruber, R. F., Matthiä, D., Lohf, H., Burmeister, S., Rafkin S. C. R., Berger, T., & Reitz, G. (2018), Energetic particle radiation environment observed by RAD on the surface of Mars during the September 2017 event, *Geophysical Research Letters*, 45, 5305-5311, <https://doi.org/10.1029/2018GL077801>.

Hassler, D.M., Zeitlin, C., Wimmer-Schweingruber, R.F., Bottcher, S., Martin, C., Andrews, J. et al. (2012). The radiation assessment detector (RAD) investigation. *Space Science Reviews*, 170, 503–558. <https://doi.org/10.1007/s11214-012-9913-1>

Hassler, D. M., Zeitlin, C., Wimmer-Schweingruber, R. F., Ehresmann, B., Rafkin, Eigenbrode, J.L. et al. (2014). Mars' surface radiation environment measured with the Mars Science Laboratory's Curiosity rover. *Science*, 343, p.1244797. <https://doi.org/10.1126/science.1244797>

Guo, J., C. Zeitlin, R. F. Wimmer-Schweingruber, D. M. Hassler, B. Heber, A. Posner, J. Kohler, S. Rafkin, B. Ehresmann, J. K. Appel, E. Bohm, S. Bottcher, S. Burmeister, D. E. Brinza, H. Lohf, C. Martin, G. Reitz (2015a). MSL-RAD Radiation Environment Measurements, *Radiation Protection Dosimetry*, **166 (1-4)**, 290-294, <https://doi.org/10.1093/rpd/ncv297>.

Guo, J., C. Zeitlin, R. F. Wimmer-Schweingruber, D. M. Hassler, B. Heber, A. Posner, J. Kohler, S. Rafkin, B. Ehresmann, J. K. Appel, E. Bohm, S. Bottcher, S. Burmeister, D. E. Brinza, H. Lohf, C. Martin, G. Reitz (2015b). Modeling the variations of Dose Rate measured by RAD during the first MSL Martian year : 2012-2014, *ApJ*, **810**, 24, DOI: [10.1088/0004-637X/810/1/24](https://doi.org/10.1088/0004-637X/810/1/24).

Guo, J., Dumbovic, M., Wimmer-Schweingruber, R. F., Temmer, M., Lohf, H., Wang, Y., Veronig, A., Hassler, D. M., Mays, L. M., Zeitlin, C., et al., Modeling the evolution and propagation of the 2017 September 9th and 10th CMEs and SEPs arriving at Mars constrained by remote-sensing and in-situ measurement, *Space Weather*, in press <https://doi.org/10.1029/2018SW001973>.

ICRP (1990). Recommendations of the International Commission on Radiological Protection. *ICRP Publication 60*, Ann. ICRP 21 (1-3).

Köhler, J., C. Zeitlin, B. Ehresmann, R.F. Wimmer-Schweingruber, D.M. Hassler, G. Reitz, D.E. Brinza, G. Weigle, J. Appel, S. Bottcher, E. Bohm, S. Burmeister, J. Guo, C. Martin, A. Posner, S. Rafkin, and O. Kortmann, 2015. "Measurements of the Neutron Spectrum in transit to Mars on the Mars Science Laboratory", *Life Sciences in Space Research*, 5, 6-12, <http://doi.org/10.1016/j.lssr.2015.03.001>.

Lee, C.O., et al. 2018. Observations and Impacts of the 10 September 2017 Solar Events at Mars: An Overview and Synthesis of the Initial Results, *Geophysical Research Letters*, submitted.

Mewaldt, R.A., D. Looper, C.M.S. Cohen, G.M. Mason, D.K. Happerty, M.I. Desai, A.W. Labrador, R.A. Leske, J.E. Mazur (2005). Solar-Particle Energy Spectra during the Large Events of October-November 2003 and January 2005. *29th International Cosmic Ray Conference, Pune (2005)*, **00**, 101-104.

NCRP (2000). National council on radiation protection and measurements, recommendations of dose limits for low earth orbit. NCRP Report 132

Rafkin, Scot C.R., Bent Ehresmann, Bent, Cary Zeitlin, Donald M. Hassler, Jingnan, Guo, Jan Kohler, Robert F. Wimmer-Schweingruber, Javier Gómez-Elvira, Ari-Matti Harri, Henrik Kahanpää, David E. Brinza, Gerald Weigle, Stephan Böttcher, Eckart Böhm, Söenke Burmeister, Cesar Martin, Güenther Reitz, Francis A. Cucinotta, Myung-Hee Kim, David Grinspoon, Mark A. Bullock, Arik Posner, and the MSL Science Team (2014). Diurnal variations of energetic particle radiation at the surface of Mars as observed by the Mars Science Laboratory Radiation Assessment Detector, *J. Geophys. Res. Planets*, **119**, 1345–1358, <http://dx.doi.org/10.1002/2013JE004525>.

Schneider, N., et al. (2018). Global Aurora on Mars during the September 2017 Space Weather Event, *Geophysical Research Letters*, 45, <https://doi.org/10.1029/2018GL077772>.

Share, G., and R. Murphy, 2018. Gamma-ray and Neutron Monitor Observations of the 2017 September 10 Solar Eruptive Event. AMS-2 Workshop #3, Washington, D.C., 24 Apr., 2018.

Smith, D. E., et al. (2001), Mars Orbiter Laser Altimeter: Experiment summary after the first year of global mapping of Mars, *J. Geophys. Res.*, **106(E10)**, 23689–23722, doi: 10.1029/2000JE001364.

Simpson, J.A. (1983). Elemental and isotopic composition of the galactic cosmic rays. *Annual Review of Nuclear and Particle Science*, 33, 323-382. <https://doi.org/10.1146/annurev.ns.33.120183.001543>

Slaba, T.C., S.R. Blattnig & F.F. Badavi (2010). Faster and more accurate transport procedures for HZETRN, *Journal of Computational Physics*, 229, 9397-9417, <https://doi.org/10.1016/j.jcp.2010.09.010>.

Wimmer-Schweingruber, R.F., J. Kohler, Donald M. Hassler, J. Guo, J. Appel, C. Zeitlin, E. Böhm, B. Ehresmann, H. Lohf, S. I. Böttcher, S. Burmeister, C. Martin, A. Kharytonov, D. E. Brinza, A. Posner, G. Reitz, D. Matthia, S. Rafkin, G. Weigle, and F. Cucinotta (2015). Zenith-Angle Dependence of the Martian Radiation Environment at Gale Crater Altitudes, *Geophys. Res. Lett.*, **42**, 10,557–10,564 (DOI:10.1002/2015GL066664).

Zeitlin, C., Hassler, D.M., Cucinotta, F.A., Ehresmann, B., Wimmer-Schweingruber, R.F., Brinza, D.E. et al. (2013). Measurements of energetic particle radiation in transit to mars on the mars science laboratory. *Science*, 340, 1080–1084. <https://doi.org/10.1126/science.1235989>

Zeitlin, C., D. M. Hassler, R. F. Wimmer-Schweingruber, B. Ehresmann, J. Appel, E. Böhm, S. Böttcher, D. E. Brinza, S. Burmeister, J. Guo, J. Köhler, H. Lohf, C. Martin, A. Posner, S. Rafkin, G. Reitz, M. Vincent, G. Weigle, Y. D. Tyler, Y. Iwata, H. Kitamura, T. Murakami (2016). Calibration Report of the RAD Instrument on the Mars Science Laboratory, *Space Science Reviews*, DOI: 10.1007/s11214-016-0303-y.

Zeitlin, C., Hassler, D.M., Guo, J., Ehresmann, B., Wimmer-Schweingruber, R.F., Rafkin, S.C. et al. (2018). Investigation of the Radiation Hazard Observed by RAD on the Surface of Mars during the Sept 2017 Solar Particle Event. *Geophysical Research Letters*, 45, <https://doi.org/10.1029/2018GL077760>.

Table 1. Dose and dose equivalent rates before, during and after the September 10, 2017 solar particle event (from Zeitlin et al. 2018)

	5 days pre-SPE (GCR only)	SPE peak period	5 days post-SPE (GCR only)
Omnidirectional dose rate* B ($\mu\text{Gy/day}$)	240	718	208
Omnidirectional dose rate E ($\mu\text{Gy/day}$)	265	588	232
$\langle Q \rangle$ (dimensionless)	2.26	1.17	2.33
Dose equivalent rate using B ($\mu\text{Sv/day}$)	543	841	485
Dose equivalent rate using E ($\mu\text{Sv/day}$)	599	688	541

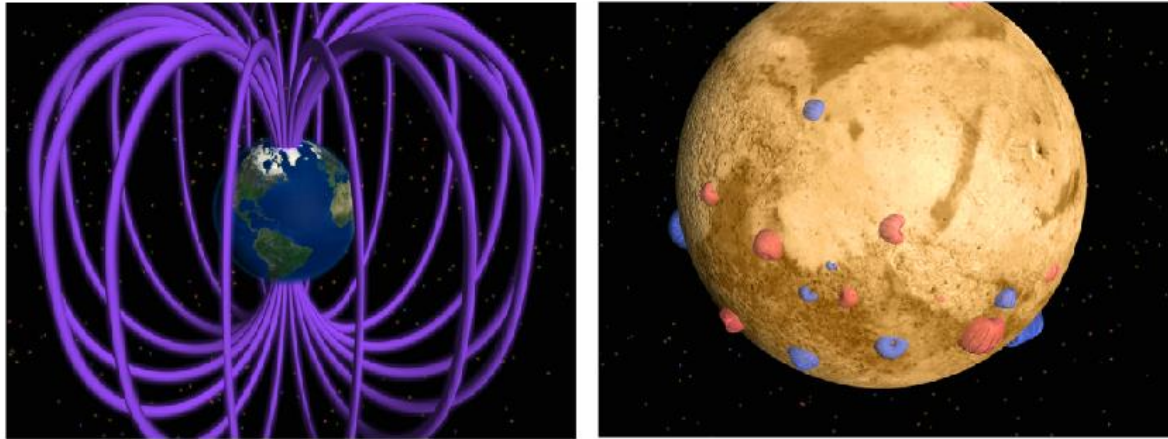


Figure 1. Cartoon illustrating the global magnetic field of Earth (left), and lack of a global magnetic field on Mars (right). This lack of a global magnetic field combined with the fact that Mars has a much thinner (~1%) atmosphere than Earth means that the surface of Mars is much more exposed to space radiation and space weather than is the surface of Earth. (Credit: MGS Magnetometer team)

Accepted Article

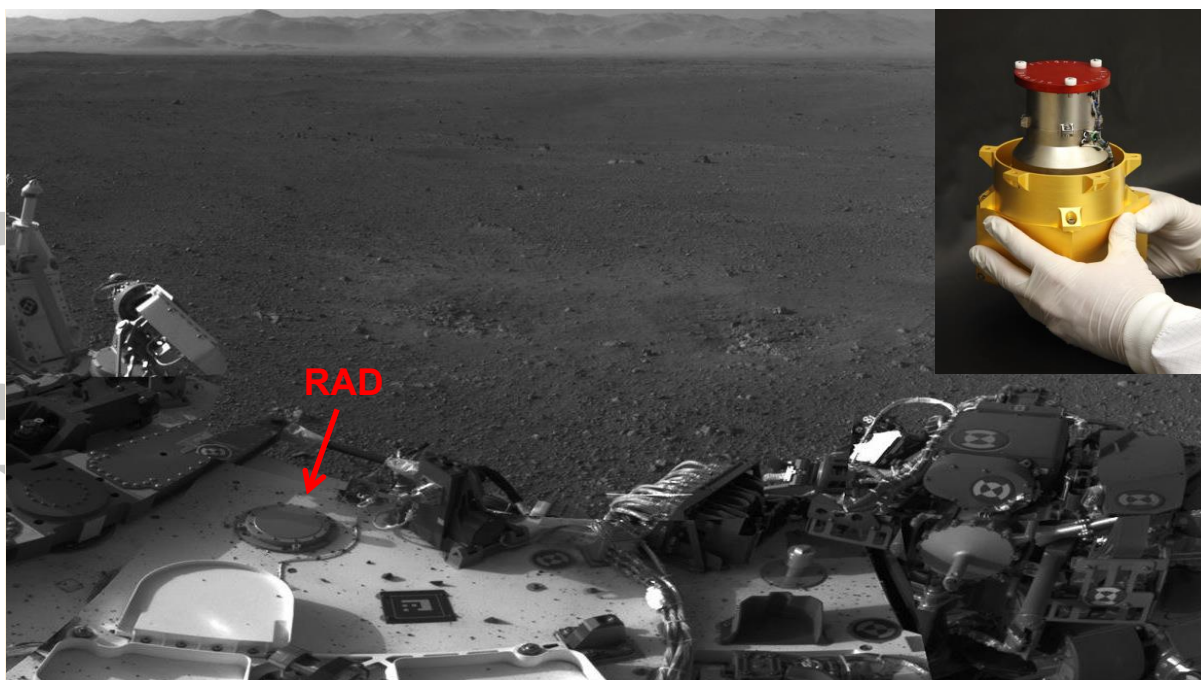


Figure 2. Photo of RAD on the Mars Science Laboratory a few days after landing on Mars on Aug. 6, 2012. The primary objective of RAD is to characterize the changing radiation environment on Mars over the solar cycle due to galactic cosmic rays & solar energetic particles.. (Credit: NASA/JPL, SwRI)

Accepted

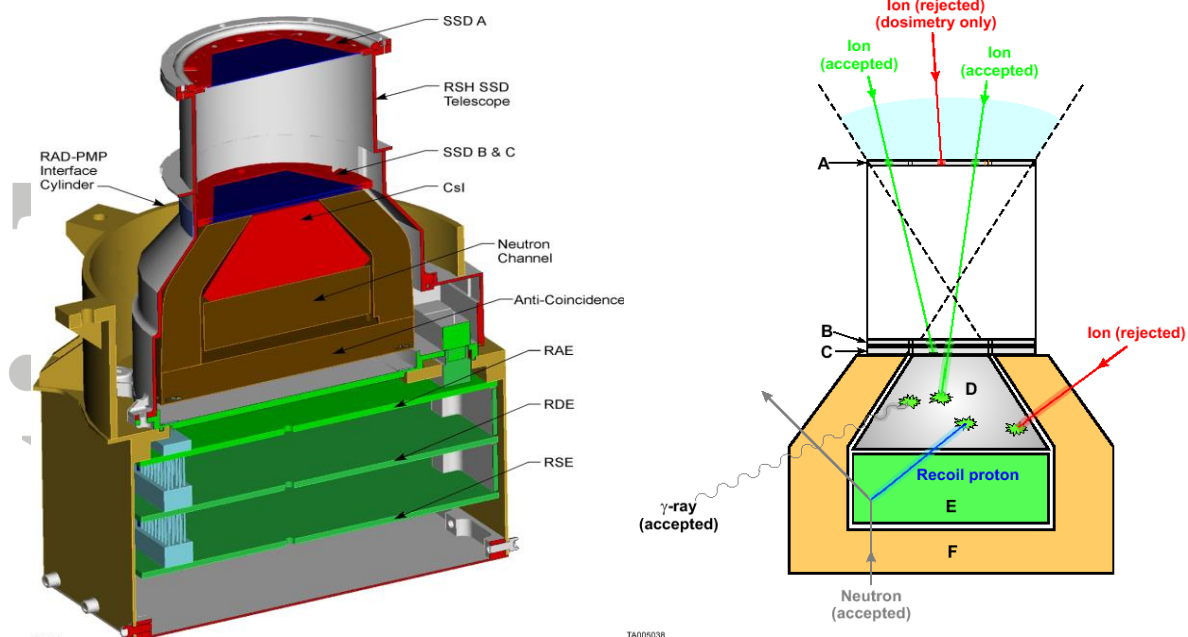


Figure 3. Cross section cartoon view of RAD (left) and schematic diagram (right) illustrating the coincidence and anti-coincidence channel concepts. The charged particle telescope is comprised of 3 silicon detectors (A, B, C), and a CsI calorimeter (D). The neutral particle subsystem is comprised of the CsI scintillator (D) and a plastic scintillator (E), surrounded by an anti-coincidence shield (F) operating in anti-coincidence mode to identify neutrons and γ -rays. Particle trajectories shown in green are considered valid events, those shown in red are rejected. RAD also has two individual dosimetry channels which measures dose rate in silicon (Detector B) and in tissue-equivalent plastic (Detector E) (Hassler et al. 2012).

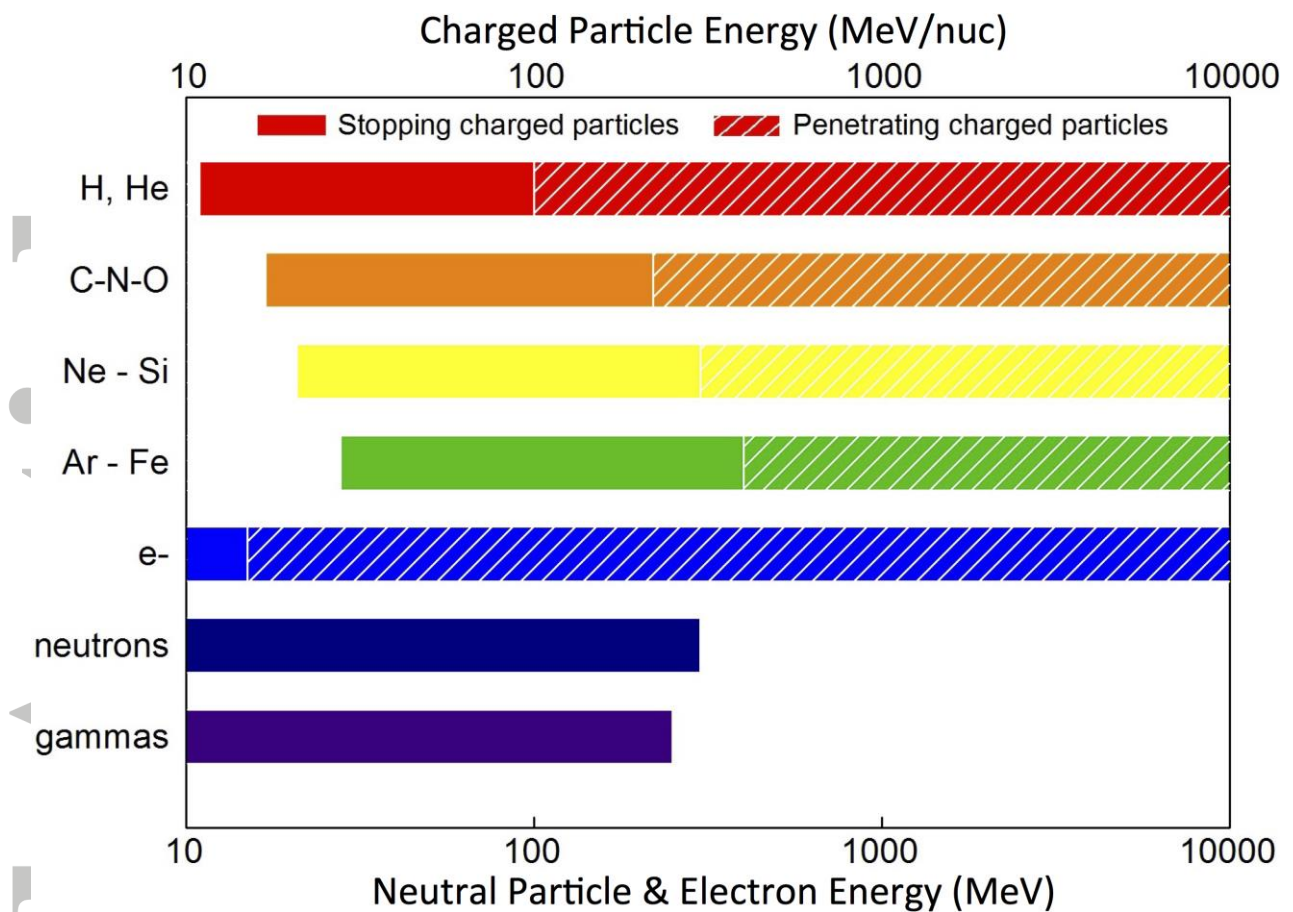


Figure 4. RAD energy range and coverage by particle type. Stopping particle energy ranges for charged particles are shown in solid colors, penetrating charged particles in striped color.

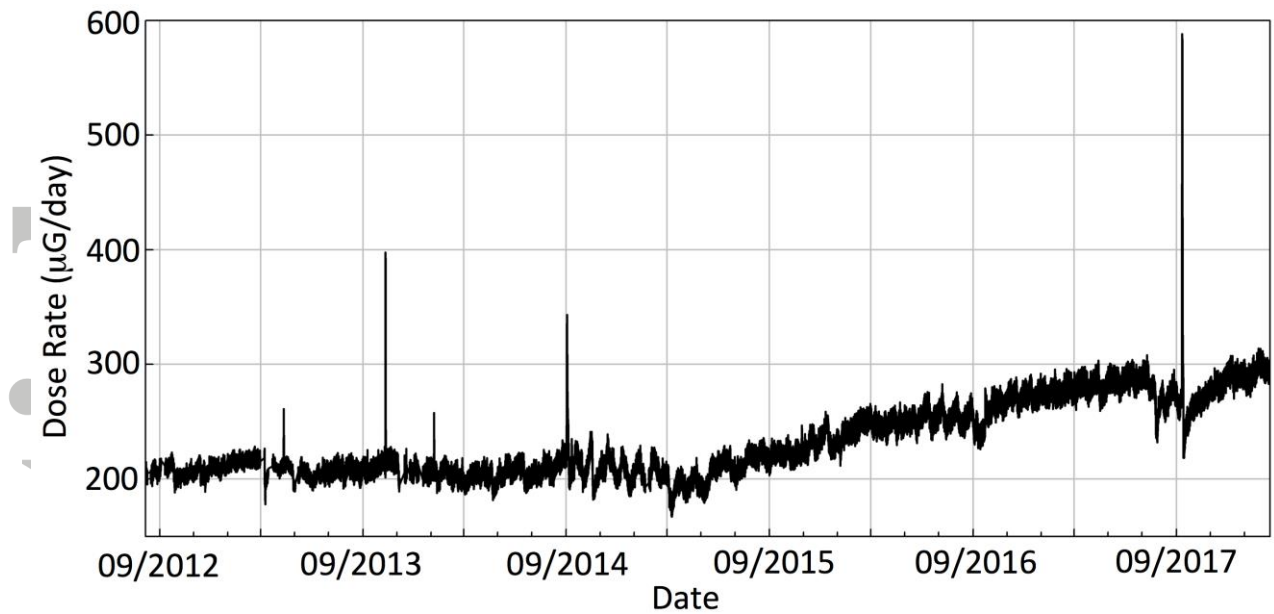


Figure 5. RAD dose rate as a function of time from Aug. 7, 2012 to Feb. 15, 2018. The dose rate has increased >50% since summer 2015 due to decreased solar activity as the Sun approaches solar minimum. RAD had observed only relatively small events until this most recent event on Sept. 10, 2017. However, it must be noted that a solar energetic particle (SEP) event must be relatively hard (>150 MeV) to make it to the surface, otherwise the only observed effect may be a Forbush decrease.

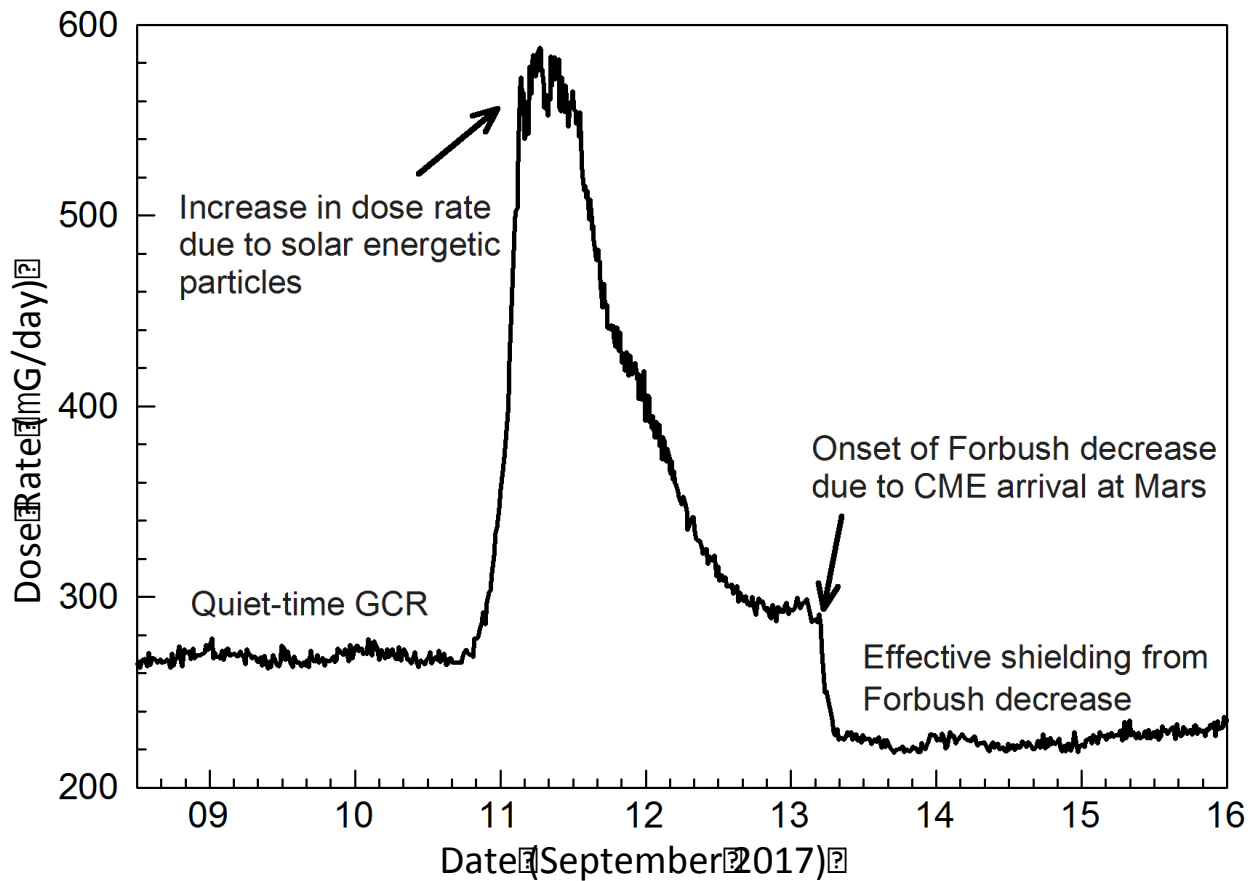


Figure 6. During the Sept. 10, 2017 SPE, RAD dose rates increased above background GCR levels by a factor of two over the course of several hours and leveled off at sustained peak rates for about 12 hours before declining over the following 36 hours. As the SEP flux was gradually declining, a shock front associated with a CME reached Mars, causing a Forbush decrease, with a sudden drop of about 15% in dose rate. The shielding of the GCR by the CME reduced their intensity below pre-event intensities.

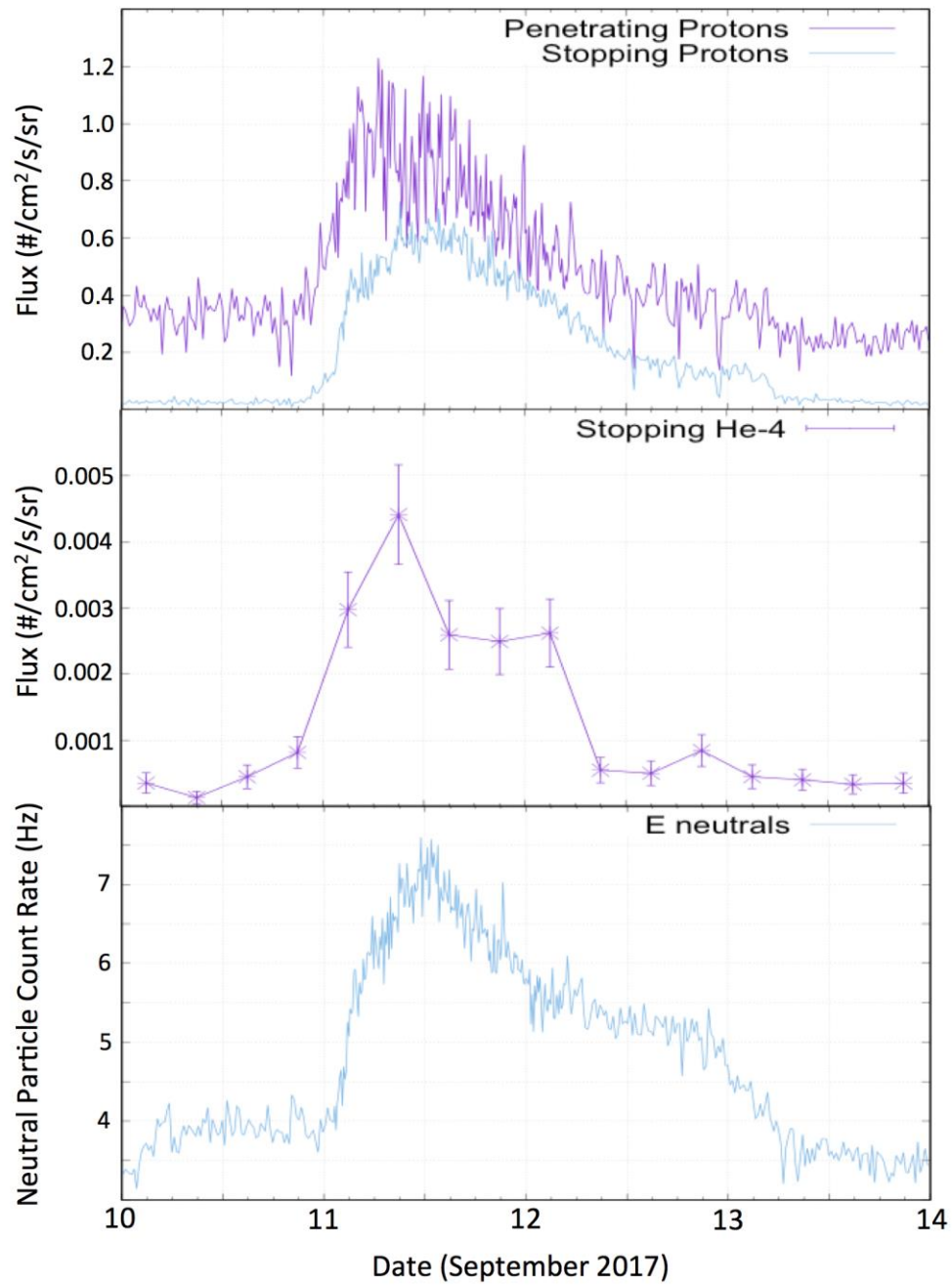


Figure 7. Integrated RAD particle flux vs time during the Sept. 10, 2017 event for stopping and penetrating protons (top), stopping ^4He (middle) and neutral particles (bottom).